Journal of Inflammation Research

Dovepress
Taylor & Francis Group

Open Access Full Text Article

ORIGINAL RESEARCH

Synthetic 1,3,6-Tri-O-Galloyl-α-D-Glucose Mimics the Hippo Pathway Inhibitor VT107 in Suppressing Concanavalin A-Induced Inflammation in Human Glioblastoma Cells

Angélique Sabaoth Konan[1], Rosalie Zilinski[1], Mirolla Tadrous[1], Alain Zgheib[1], Roger Gaudreault[2], Borhane Annabi[1]

[1]Laboratoire d'Oncologie Moléculaire, Chaire en Prévention et Traitement du Cancer, Université du Québec à Montréal, Montréal, QC, H3C 3P8, Canada; [2]Département de Chimie, Université du Québec à Montréal, Montréal, QC, H3C 3P8, Canada

Correspondence: Borhane Annabi, Laboratoire d'Oncologie Moléculaire, Université du Québec à Montréal, C.P. 8888, Succ. Centre-ville, Montréal, Québec, H3C 3P8, Canada, Tel +1 514 987-3000 ext. 7610, Email annabi.borhane@uqam.ca

Journal of Inflammation Research downloaded from https://www.dovepress.com/
For personal use only.

Background: Glioblastoma (GBM) is the most aggressive primary tumor of the adult central nervous system, not only characterized by rapid proliferation and diffuse brain infiltration but also by a pronounced pro-inflammatory microenvironment that fuels tumor progression and therapeutic resistance. Current standard-of-care, surgical resection followed by radiotherapy and chemotherapy, offers limited survival benefit, partly due to inflammation-driven invasion and immune evasion. The Hippo signaling pathway, a critical regulator of cell proliferation, apoptosis, and tissue homeostasis, has recently been implicated in inflammatory signaling, making it an attractive therapeutic target.

Purpose: In this study, we investigated the anti-inflammatory and anti-invasive properties of 1,3,6-tri-O-galloyl-α-D-glucose (αTGG), the α-anomer of βTGG from *Terminalia chebula*, in comparison with pharmacological Hippo pathway inhibitors IAG933, VT107, and GNE7883.

Results: To mimic the inflammatory milieu associated with GBM, U87 cells were treated with Concanavalin A (ConA), which induced phosphorylation of ERK and IκB, key mediators of MAPK and NF-κB inflammatory pathways. Both αTGG and Hippo pathway inhibitors effectively suppressed these phosphorylation events, with VT107 showing the strongest effect. ConA exposure downregulated Hippo pathway downstream effectors (*AXL, CTGF, CYR61*) in a TEAD-dependent manner, highlighting the interplay between Hippo signaling and inflammatory transcriptional control. Importantly, αTGG and VT107 also significantly attenuated ConA-induced activation of proMMP-2 to MMP-2 and reduced the expression of multiple pro-inflammatory mediators, including *COX2, CCL22, CCR2, CCR4, CXCL10, CXCL12, CXCR1, FASLG, IFNG, IL13*, and *IL17A*.

Conclusion: These findings underscore the dual anti-inflammatory and anti-invasive actions of αTGG, positioning it as a promising candidate for targeting inflammation-driven GBM progression through modulation of Hippo pathway activity.

Keywords: Concanavalin A, glioblastoma, hippo pathway inhibitors, inflammation, 1,3,6-tri-O-galloyl-α-D-glucose

Introduction

Neuroinflammation is a central driver of glioblastoma (GBM) progression and aggressiveness,[1,2] shaping a chronically inflamed tumor microenvironment (TME) that promotes growth, angiogenesis, invasion, and therapy resistance.[3] Persistent release of pro-inflammatory cytokines (for example, IL-1β, IL-6, IL-8, TNF-α) from tumor and infiltrating immune cells disrupts the blood-brain barrier, enhances immune evasion, and fuels tumor cell proliferation and invasion.[4] Key inflammatory signaling cascades, including NF-κB, MAPK, STAT3, and Hippo, sustain this pro-tumorigenic milieu and blunt responses to immunotherapy and conventional treatments.[5–7] Targeting inflammation therefore offers a twofold

Received: 19 September 2025
Accepted: 25 November 2025
Published: 19 December 2025

© 2025 Konan et al. This work is published and licensed by Dove Medical Press Limited. The full terms of this license are available at https://www.dovepress.com/terms.php and incorporate the Creative Commons Attribution – Non Commercial (unported, v4.0) License (http://creativecommons.org/licenses/by-nc/4.0/). By accessing the work you hereby accept the Terms. Non-commercial uses of the work are permitted without any further permission from Dove Medical Press Limited, provided the work is properly attributed. For permission for commercial use of this work, please see paragraphs 4.2 and 5 of our Terms (https://www.dovepress.com/terms.php).

opportunity: to directly suppress tumor-promoting signals, reducing invasiveness and matrix remodeling, and to reprogram the immune microenvironment toward anti-tumor activity.[8,9]

Pharmacological approaches are increasingly directed at these inflammatory axes: small-molecule inhibitors of NF-κB/STAT3 and Hippo pathway modulators (eg, GNE7883, IAG933, verteporfin and related TEAD inhibitors) show anti-proliferative, anti-vasculogenic mimicry, and anti-inflammatory effects in preclinical GBM models;[10–13] repurposed anti-inflammatory drugs including minocycline, celecoxib and CSF-1R-mediated blockade of tumor-associated macrophage activity are also under evaluation to reprogram tumor-associated inflammation.[14–16] Nowadays, immunomodulatory therapies, such as checkpoint inhibitors, are also being combined with anti-inflammatory agents to overcome immune suppression. Natural compounds like curcumin are gaining attention for their dual anti-inflammatory and anti-invasive properties.[17,18] Collectively, they may represent a shift toward integrated, inflammation-targeted GBM therapy.

The Hippo pathway, through its effectors YAP and TAZ, is a key regulator of proliferation, apoptosis, and tissue homeostasis whose dysregulation promotes GBM progression.[19] Dephosphorylated YAP/TAZ translocate to the nucleus and drive genes that enhance invasion and inflammatory signaling, including upregulation of MMPs and pro-inflammatory cytokines.[6,20,21] This activity accelerates extracellular matrix degradation, immune cell recruitment, and a tumor-supportive, immune-suppressive microenvironment, with YAP/TAZ functionally interacting with NF-κB and STAT3 to amplify inflammation.[22] Hippo dysregulation also fosters apoptosis resistance and immune evasion,[23] while pharmacological YAP/TAZ or YAP/TEAD inhibition reduces inflammatory/invasive marker expression in GBM models.[24,25] Targeting Hippo signaling therefore offers a focused strategy to blunt tumor-promoting inflammation and invasion.

Here, we tested the anti-inflammatory activity of 1,3,6-tri-O-galloyl-α-D-glucose (αTGG), the α-anomer of βTGG from *Terminalia chebula*, and compared its effects with Hippo pathway inhibitors IAG933, VT107 and GNE7883 in a human GBM-derived cell line, focusing on inflammatory readouts and invasive phenotypes.

Methods

Reagents and Cells

Sodium dodecyl sulfate (SDS), Concanavalin A (ConA) and bovine serum albumin (BSA) were obtained from Sigma-Aldrich Corp. (St. Louis, MO, USA). The Hippo pathway inhibitors, IAG933, VT107, and GNE7883, were sourced from Chemietek (Indianapolis, IN, USA). αTGG was generously provided by Dr. Yann Pauvert.[26] Eagle's Minimum Essential Medium (EMEM) for cell culture was purchased from Wisent (320–005 CL). Electrophoresis reagents were acquired from Bio-Rad Laboratories (Hercules, CA, USA). The HyGLO™ Chemiluminescent HRP Antibody Detection Reagents were supplied by Denville Scientific Inc. (Metuchen, NJ, USA). Protein quantification was performed using the Micro BCA™ Protein Assay Kit from Pierce (Thermo Fisher Scientific, Waltham, MA, USA). Primary antibodies targeting GAPDH (D4C6R – CAT# 97166 S), IκBα (4814S), phospho-IκBα Ser32/36 (9246S), p44/42 MAPK (ERK1/2), and phospho-p44/42 MAPK (ERK1/2) were purchased from Cell Signaling Technology (Danvers, MA, USA). Secondary HRP-conjugated donkey anti-rabbit and anti-mouse IgG antibodies were obtained from Jackson ImmunoResearch Laboratories (West Grove, PA, USA). Human U87 glioblastoma (GBM)-derived cells were sourced from the American Type Culture Collection (ATCC; Manassas, VA, USA). Cells were cultured under subconfluent conditions and passaged twice weekly at a 1:2 ratio. Incubation and treatments were carried out at 37°C in a humidified atmosphere containing 5% CO_2 as previously described.[27]

Transfection Method and RNA Interference

For gene silencing experiments, U87 cells were transiently transfected with small interfering RNA (siRNA) using Lipofectamine 2000 (Thermo Fisher Scientific, Waltham, MA, USA) as the transfection reagent. Silencing was carried out using 20 nM siRNA targeting *YAP1* (Hs_YAP1_5 siRNA, SI02662954), *TEAD1* (Hs_TEAD1_5 siRNA, SI04181261), or a non-targeting scrambled control (AllStar Negative Control siRNA, 1027281). All siRNA sequences, including the mismatch controls, were synthesized by QIAGEN and annealed to form duplexes prior to transfection. The efficiency of gene knockdown was evaluated by RT-qPCR.

Total RNA Extraction, cDNA Synthesis, and Real-Time Quantitative PCR

Total RNA was extracted from U87 GBM cell monolayers using TRIzol reagent, following the manufacturer's protocol (Life Technologies, Gaithersburg, MD, USA). RNA concentration was determined using a NanoPhotometer P330 (Implen), and 2 µg of RNA were reverse-transcribed into complementary DNA (cDNA) using the High-Capacity cDNA Reverse Transcription Kit (Applied Biosystems, Foster City, CA, USA). Quantitative PCR reactions were prepared using gene-specific primer sets and SsoFast EvaGreen Supermix (Bio-Rad; 1725204). All primers were obtained from QIAGEN as QuantiTect Primer Assays for the following genes: *YAP1* (Hs_YAP1_1_SG, QT00080822), *TEAD1* (Hs_TEAD1_1_SG, QT00000721), *CTGF* (Hs_CTGF_1_SG, QT00052899), *CYR61* (Hs_CYR61_1_SG, QT00003451), *AXL* (Hs_AXL_1_SG, QT00067725), *NF2* (Hs_NF2_va.1_SG, QT01004934), *COX-2* (Hs_PTGS2_1_SG, QT00040586), *IL6* (Hs_IL6_1_SG, QT00083720), *GAPDH* (Hs_GAPDH_1_SG, QT00079247), and *PPIA* (Hs_PPIA_4_SG, QT01866137). Gene expression levels were quantified RT-qPCR using the CFX Connect system (Bio-Rad) and analyzed with Bio-Rad CFX Manager Software version 3.0. Relative expression of target genes was normalized to the housekeeping genes *GAPDH* and *PPIA* using the $2^{-\Delta\Delta Cq}$ method.

PCR Arrays

Preconfigured RT^2 Profiler PCR Arrays for Human Inflammatory Cytokines and Receptors (PAHS-011ZD) and Human Cancer Inflammation and Immunity Crosstalk (PAHS-181Z) were purchased from QIAGEN and used according to the manufacturer's instructions. Prior to reverse transcription, genomic DNA was removed from the RNA samples, total RNA converted into cDNA and relative expression levels of 141 genes and internal controls quantified and analysed as previously described.[27] For data visualization, genes were considered upregulated when fold regulation exceeded +2, and downregulated when fold regulation was below −2, based on the overall expression profile.

Protein-to-Protein Interactions

Protein-protein interaction (PPI) networks were constructed using the STRING database (version 11; https://www.string-db.org), applying a minimum confidence score threshold of 0.4.[28] To enhance the readability of the network visualizations, the maximum number of displayed interactions per protein was limited to 10.

Western Blot

Protein samples (10–20 µg) from total cell lysis were separated by SDS-polyacrylamide gel electrophoresis (SDS-PAGE) , followed by electrotransfer onto low-fluorescence polyvinylidene difluoride (PVDF) membranes, and immunodetection were performed as previously described.[27]

Zymography

Gelatin zymography of the collected conditioned culture media was employed to evaluate the extracellular gelatinolytic activity of pro-MMP-9, pro-MMP-2, and active MMP-2 as previously described.[29]

Statistical Data Analysis

All statistical analyses were performed using GraphPad Prism 7 (GraphPad Software, San Diego, CA; https://www.graphpad.com). Data are presented as mean ± standard error of the mean (SEM) from at least three independent experiments, unless otherwise indicated. Comparisons between two groups were assessed using the Mann–Whitney *U*-test followed by Dunn Tukey's post hoc test (for data with more than three groups). For Figure 1B, statistical significance was determined using two-way ANOVA. A *p*-value less than 0.05 (*) was considered statistically significant.

Results

Time-Dependent Inhibition of Concanavalin A-Induced Phosphorylation of ERK and IκB by αTGG in Human U87 Glioblastoma Cells

Concanavalin A (ConA) is widely used in experimental immunology and cell biology as a pro-inflammatory pharmacological tool.[30–32] Here, we first wished to assess and optimize U87 GBM cell responsiveness to ConA. Serum-starved

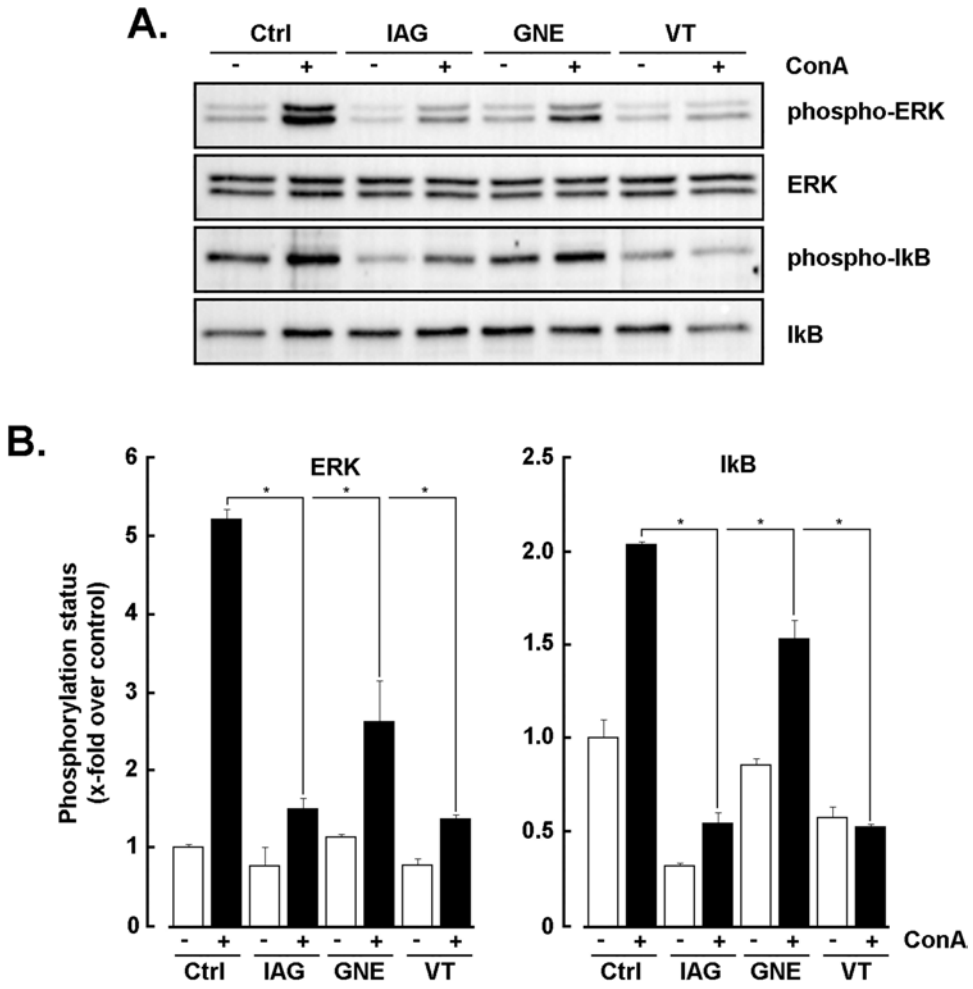

Figure 1 *Hippo pathway inhibitors alter the Concanavalin A-induced phosphorylation of ERK and IκB in human U87 glioblastoma cells*. Serum-starved human U87 glioblastoma cells were treated with 30 μg/mL Concanavalin A (ConA) for 5 min in the absence or presence of 3 μM IAG933 (IAG), GNE7883 (GNE), or VT107 (VT). (**A**) Protein cell lysates were harvested and processed for immunoblotting as described in the Methods section, to detect the phosphorylation status of ERK and of IκB. (**B**) Densitometric analysis was performed and phosphorylation status expressed as the extent of phospho-ERK/ERK or phosphor-IκB/IκB ratios over untreated control cells. Data points are the means ± SEM of 3 independent experiments.

cells were treated with 30 μg/mL ConA in the absence or presence of 30 μM αTGG, and phosphorylation of ERK and of IκB found to be triggered (Figure 2A). Densitometric analysis shows that phosphorylation of ERK peaked at 5 minutes, whereas that of IκB did at 2 minutes (Figure 2B). In both conditions, αTGG treatment prevented these increases.

Dose-Dependent Inhibition of Concanavalin A-Induced Phosphorylation of ERK and IκB by αTGG in Human U87 Glioblastoma Cells

We next screened for the optimal αTGG-to-ConA capacity of cell signaling inhibition (Figure 3A). Serum-starved human U87 GBM cells were therefore treated with increasing concentrations of ConA for 5 min in the absence or presence of 30 μM αTGG and found to significantly inhibit ERK phosphorylation starting at 3 μg/mL ConA (Figure 3B, left panel). Similarly, IκB phosphorylation was also tested at 2 minutes stimulation with ConA, and αTGG found to prevent phosphorylation starting at 1 μg/mL ConA (Figure 3B, right panel).

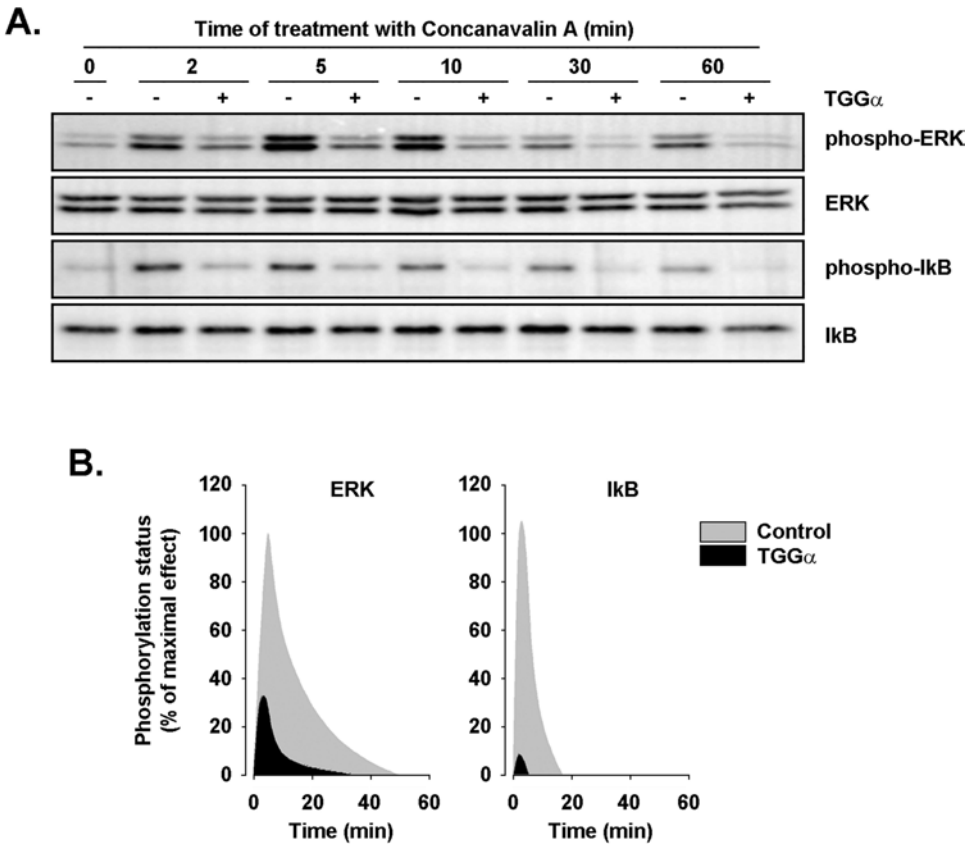

Figure 2 *Time-dependent inhibition of Concanavalin A-induced phosphorylation of ERK and IκB by αTGG in human U87 glioblastoma cells.* Serum-starved human U87 glioblastoma cells were treated with 30 µg/mL Concanavalin A (ConA) for the indicated time in the absence or presence of 30 µM αTGG. (**A**) Protein cell lysates were harvested and processed for immunoblotting as described in the Methods section, to detect the phosphorylation status of ERK and of IκB. (**B**) Densitometric analysis was performed and phosphorylation status expressed as the maximal value of phospho-ERK/ERK or phosphor-IκB/IκB ratios for control (grey shades) vs αTGG (black shades). Western blot and densitometric analysis are representative of 3 independent experiments.

Dose-Dependent Inhibition of Concanavalin A-Induced Snail, COX2, and Activation of proMMP-2 by αTGG in Human U87 Glioblastoma Cells

Downstream induction by ConA of inflammatory and EMT biomarkers expression of respectively COX2 and Snail, and impact of αTGG, was next assessed. Serum-starved human U87 GBM cells were treated with increasing concentrations of αTGG in the absence or presence of ConA for 24 hours. The expression of both Snail and COX2 was effectively triggered by ConA and found to be prevented by αTGG (Figure 4A). Expression of GAPDH in the cell lysates, which served as a loading control, remained unaltered. Along with the above inhibitions of downstream inflammatory biomarkers in ConA-primed U87 cells, αTGG capacity to further inhibit proMMP-2 activation by ConA was examined as previously reported.[33,34] Conditioned media was isolated from the respective conditions and αTGG found to dose-dependently alter the extent of ConA-induced proMMP-2 activation as assessed by gelatin zymography (Figure 4B). Given the long-term treatment, cell viability was assessed and found unaltered upon increasing αTGG treatment concentrations (Figure 4C).

Differential YAP/TEAD Control of Concanavalin A-Mediated Regulation of Hippo Pathway Downstream Effectors

We next wished to address the signaling crosstalk that would inter-relate the Hippo pathway to the pharmacological effects of ConA. Serum-starved human U87 GBM cells were treated with the indicated concentrations of ConA for 24 hours, total RNA was extracted and RT-qPCR performed as described in the Methods section. ConA dose-dependently triggered the expression of *COX2* and *IL6* as previously reported (Figure 5A, left top and bottom panels).[35] Interestingly,

https://doi.org/10.2147/JIR.S565721

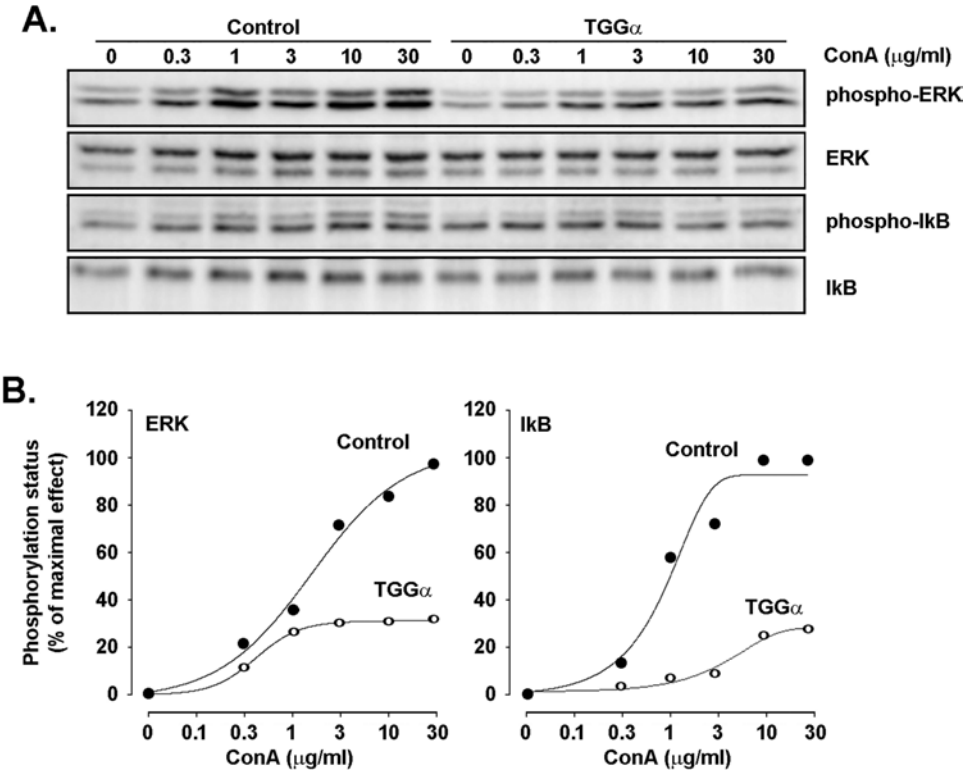

Figure 3 *Dose-dependent inhibition of Concanavalin A-induced phosphorylation of ERK and IκB by αTGG in human U87 glioblastoma cells*. Serum-starved human U87 glioblastoma cells were treated with the indicated concentrations of Concanavalin A (ConA) for 5 min in the absence or presence of 30 μM αTGG. (**A**) Protein cell lysates were harvested and processed for immunoblotting as described in the Methods section, to detect the phosphorylation status of ERK and of IκB. (**B**) A representative densitometric analysis was performed and phosphorylation status expressed as the maximal value of phospho-ERK/ERK or phosphor-IκB/IκB ratios for control (closed circles) vs αTGG (open circles). Western blot and densitometric analysis are representative of 3 independent experiments.

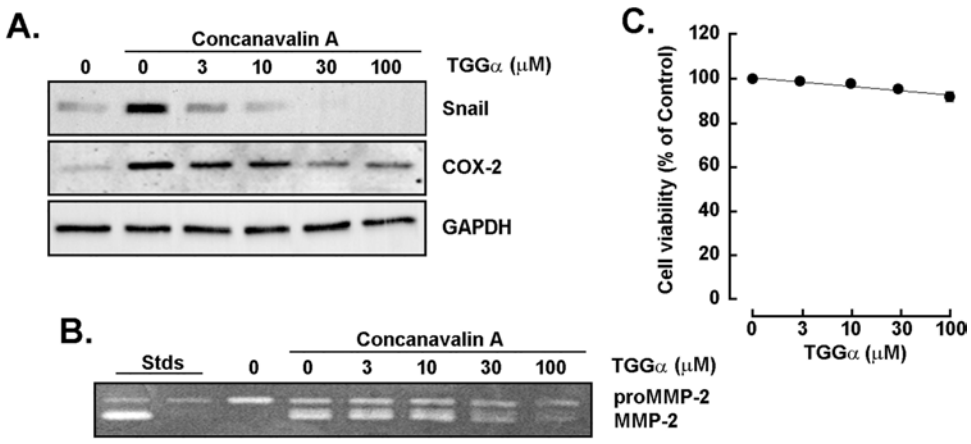

Figure 4 *Dose-dependent inhibition of Concanavalin A-induced Snail, COX2, and activation of proMMP-2 by αTGG in human U87 glioblastoma cells*. Serum-starved human U87 glioblastoma cells were treated with the indicated concentrations of αTGG in the absence or presence of 30 μg/mL Concanavalin A (ConA) for 24 hours. (**A**) Protein cell lysates were harvested and processed for immunoblotting as described in the Methods section, to detect the expression levels of Snail and COX2. GAPDH served as a loading control. (**B**) A gelatin zymography was performed using the conditioned media isolated from the respective conditions as described in the Methods section to assess the effect of αTGG on the extent of ConA-induced proMMP-2 activation. (**C**) U87 glioblastoma cells were treated with the indicated concentrations of αTGG for 24 hours. Cell viability was evaluated for each concentration using the Trypan Blue exclusion assay and a TC20 Automated Cell Counter (Biorad). Data are representative of two independent experiments.

it also decreased the expression of downstream Hippo pathway effectors *AXL, CTGF*, and *CYR61* gene expression, while inducing that of *NF2* (Figure 5A). In order to next assess the involvement of the upstream control exerted by YAP1 and TEAD, transient gene silencing was performed and extent and specificity of gene repression confirmed (Figure 5B).

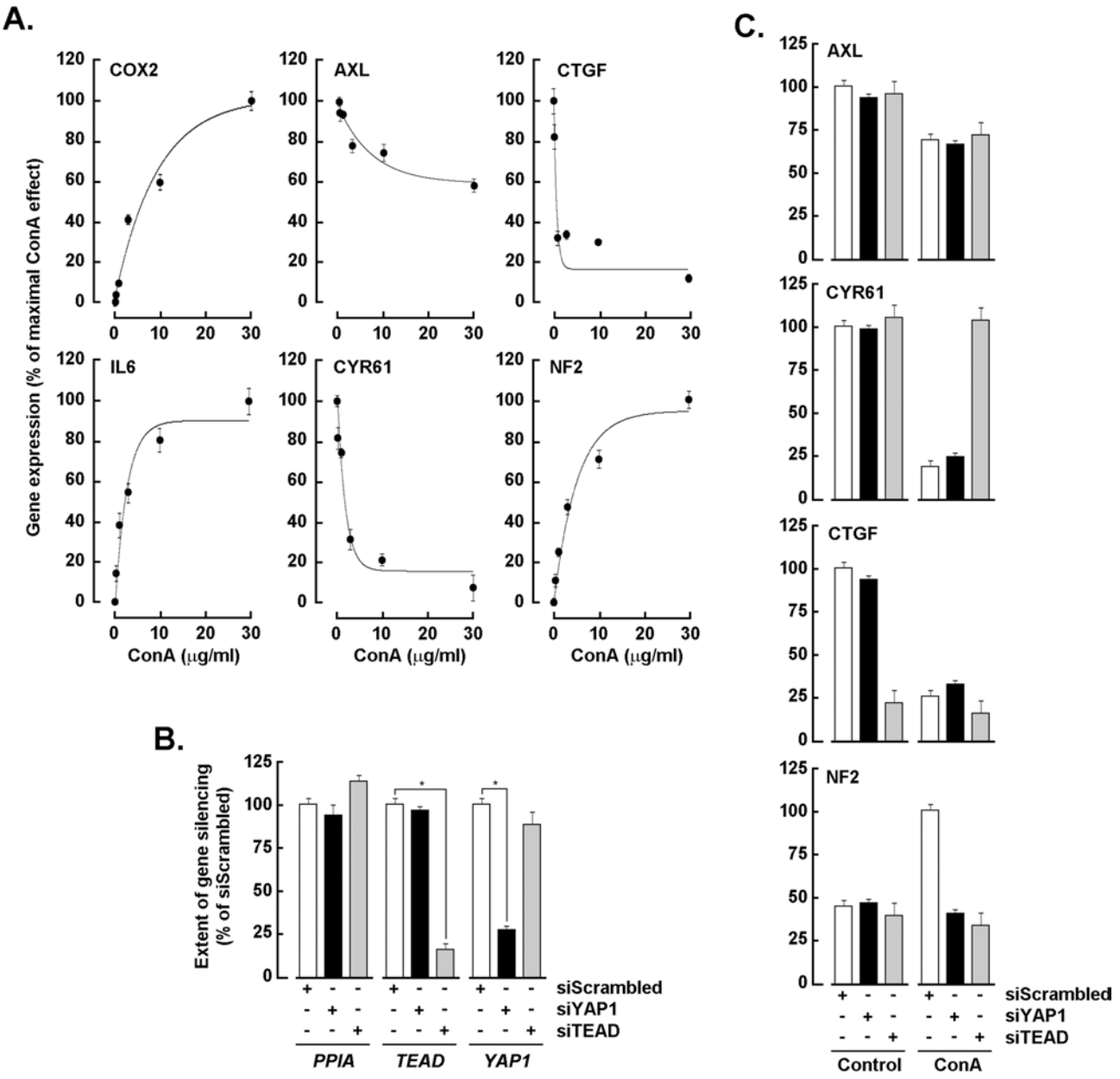

Figure 5 *Differential YAP/TEAD control of Concanavalin A-mediated regulation of Hippo pathway downstream effectors*. Serum-starved human U87 glioblastoma cells were treated with the indicated concentrations of ConA for 24 hours, total RNA was extracted and RT-qPCR performed as described in the Methods section. (**A**) Gene expression of inflammatory (*COX2, IL6*) and downstream Hippo pathway effectors (*AXL, CRGF, CYR61*, and *NF2*). (**B**) Transient gene silencing of YAP1 and TEAD was performed and extent and specificity of gene repression compared to *PPIA*. (**C**) Impact of YAP1 and TEAD silencing on ConA-mediated effects on downstream Hippo pathway effectors. Data points are the means ± SEM of triplicates from independent experiments.

Interestingly, YAP1 and TEAD silencing prevented the effects of ConA on *NF2*, while neither reversed the effects on *AXL* or *CTGF* (Figure 5C). On the other hand, only TEAD appeared to control ConA-mediated *CYR61* gene expression, while basal levels of CTGF in untreated cells also appeared to be decreased (Figure 5C). ConA-mediated downregulation of *CTGF, CYR61*, and *AXL* gene expression is consistent with activation of the Hippo signaling pathway.[36,37] Hippo pathway pharmacological targeting was next assessed. Knockdown efficiency was assessed here by qPCR and is reported as mRNA reduction. We did not obtain protein-level confirmation for the targeted gene and therefore cannot assume complete loss of protein function.

https://doi.org/10.2147/JIR.S565721

Hippo Pathway Inhibitors Alter the Concanavalin A-Induced Phosphorylation of ERK and IκB in Human U87 Glioblastoma Cells

Capacity of Hippo pathway inhibitors IAG933, GNE7883, and VT107 was next tested to assess their impact on signal transducing events triggered by ConA. Serum-starved human U87 GBM cells were treated with ConA for 5 min in the absence or presence of 3 μM IAG933 (IAG), GNE7883 (GNE), or VT107 (VT) respectively (Figure 1A). It was found that the phosphorylation status of ERK (Figure 1B, left panel, black bars) and of IκB (Figure 1B, right panel, black bars) in ConA-primed cells was significantly reduced by all three inhibitors, similarly to the impact of αTGG (Figures 2 and 3). VT107 was found to be the most effective inhibitors and was next further characterized.

The Hippo Pathway Inhibitor VT107 Alters Dose-Dependently the Concanavalin A-Induced Phosphorylation of ERK and IκB in Human U87 Glioblastoma Cells

In order to further assess the cell signaling impact of VT107, serum-starved U87 GBM cells were treated with ConA for 5 min (ERK) or 2 min (IκB) in the absence or presence of increasing concentrations of VT107 (Figure 6A, VT). Phosphorylation status of ERK (Figure 6B, left panel) and of IκB (Figure 6B, right panel) was both inhibited by VT107 with an IC_{50} of 0.72 and 0.51 μM respectively against ERK and IκB phosphorylation. Conditioned media was further collected and impact of VT107 against ConA-mediated proMMP-2 activation as assessed by gelatin zymography as described in the Methods section. Along with the above demonstrated cell signaling inhibitory impact, VT107 was further found to prevent proMMP-2 activation into MMP-2 (Figure 6C).

The Hippo Pathway Inhibitor VT107 and αTGG Share a Common Anti-Inflammatory Molecular Signature in Concanavalin A-Primed Human U87 Glioblastoma Cells

Given the evident cell signaling inhibitory profiles and shared capacity to alter downstream events from ConA-primed cells between αTGG and the three Hippo pathway inhibitors tested herein, we next proceeded with a transcriptomic gene array screen of inflammatory-associated biomarkers using panels of 141 genes as described in the Methods section. Serum-starved human U87 GBM cells were treated for 24 hours with ConA, total RNA extracted and gene expression assessed by RT-qPCR. ConA was effectively found to trigger, among the genes investigated, the expression of 41 genes (Figure 7A, green). These included members of the CXCL (*CXCL2, CXCL9, CXCL10, CXCL11, CXCL12, CXCL13*), CXCR (*CXCR1, CXCR2*, and *CXCR4*), CCL (*CCL16, CCL17, CCL22, CCL28*, and *CCL3*), CCR (*CCR2, CCR3, CCR4*, and *CCR6*), and some interleukins/interleukin receptor (*IL9, IL10, IL13, IL17A, IL17C, IL17F, IL23A, IL33, IL1R1, IL1RN*) (Supplemental Table 1). Altogether, this highlights activation of immune-related pathways, cytokine signaling, and chemokine receptor expression, and suggests that ConA treatment triggers a robust immunomodulatory response in U87 cells, potentially involving inflammatory signaling and tumor microenvironment remodeling. In addition, 17 genes were concomitantly downregulated upon ConA treatment (Supplemental Table 1). Among those genes included *TLR3, IL5, CCL2, CXCL1*, and *GBP1*, reflecting a shift in immune response and reduced inflammatory signaling following ConA treatment. Next, the 10 commonly shared genes which expression was triggered by ConA, and that was altered by treatment with all three Hippo pathway inhibitors tested, were compared to the inhibitory effects of αTGG. It was found that the best correlation existed when αTGG was compared to VT107 ($r^2 = 0.87$), while no correlation was found when αTGG effects were compared to those of either GNE7883 or IAG933 (Figure 7B). Protein-to-protein interaction network of the 10 commonly shared and downregulated genes between all the inhibitors tested in ConA-treated cells was determined with STRING and confirms the predicted inter-relationship they have between them.

Discussion

In this study, we sought to validate and optimize the responsiveness of U87 GBM cells to ConA, with the goal of characterizing inflammation-related molecular events that may contribute to the TME. ConA indeed reliably modeled inflammatory signaling in U87 GBM cells by activating diverse signaling pathways across multiple cell types[30–32] including ERK and NF-κB/IκB pathways and inducing downstream inflammatory and invasion-associated markers such as Snail, COX2, proMMP-2. Furthermore, transcriptomic profiling revealed induction of cytokine transcripts (*IFNG,*

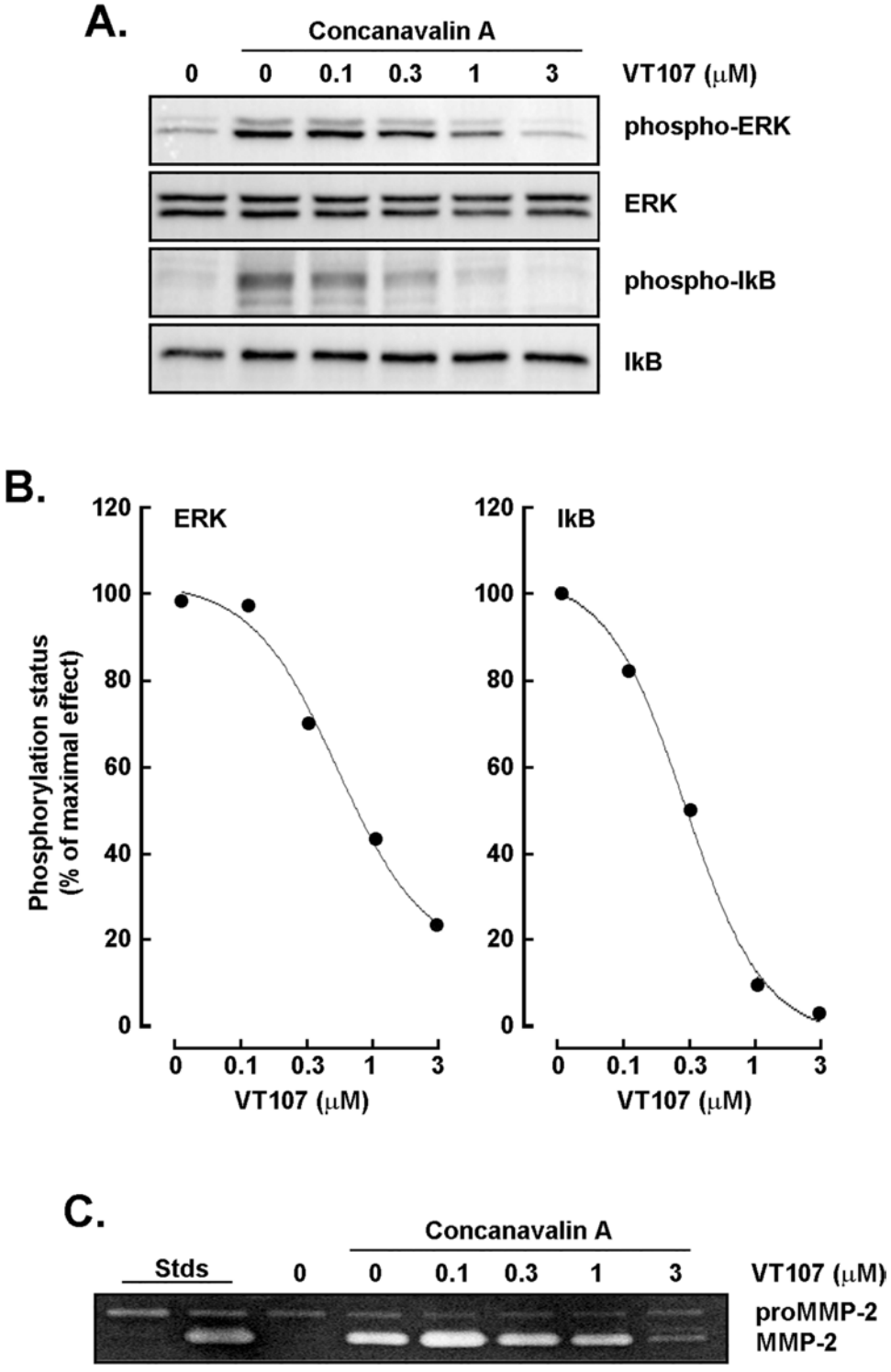

Figure 6 *The Hippo pathway inhibitor VT107 alters dose-dependently the Concanavalin A-induced phosphorylation of ERK and IκB in human U87 glioblastoma cells*. Serum-starved human U87 glioblastoma cells were treated with 30 μg/mL Concanavalin A (ConA) for 5 min in the absence or presence of the indicated concentrations of VT107 (VT). (**A**) Protein cell lysates were harvested and processed for immunoblotting as described in the Methods section, to detect the phosphorylation status of ERK and of IκB. (**B**) A representative densitometric analysis was performed and phosphorylation status expressed as the percent of phospho-ERK/ERK or phospho-IκB/IκB ratios of ConA-treated cells. Western blot and densitometric analysis are representative of 3 independent experiments. (**C**) Conditioned media was collected and gelatin zymography performed as described in the Methods section to monitor the impact of VT107 on proMMP-2 activation.

https://doi.org/10.2147/JIR.S565721

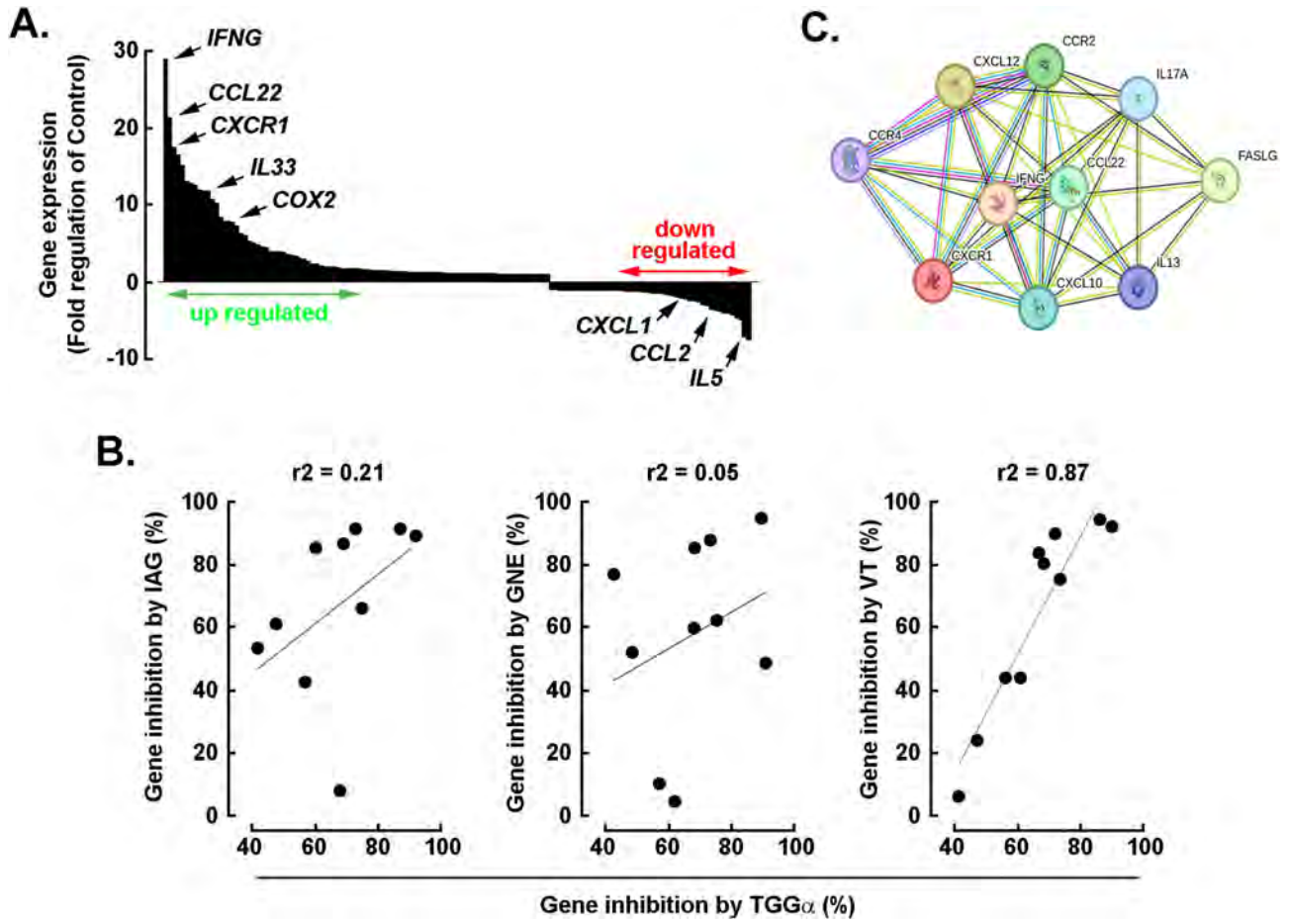

Figure 7 *The Hippo pathway inhibitor VT107 and αTGG share a common anti-inflammatory molecular signature in Concanavalin A-primed human U87 glioblastoma cells.* (**A**) Serum-starved human U87 glioblastoma cells were treated for 24 hours with 30 µg/mL Concanavalin A (ConA), total RNA extracted and processed for a gene array screen of 141 inflammatory-associated genes as described in the Methods section by RT-qPCR. (**B**) Serum starved cells were similarly treated with ConA in the presence of 1 µM of either IAG933 (IAG), GNE7883 (GNE) or VT107 (VT) for 24 hours and extent of inhibition of the 10 most induced common genes assessed and correlated to that of 30 µM αTGG. (**C**) Protein-to-protein interaction network of the 10 commonly shared and downregulated genes between all the inhibitors tested in ConA-treated cells as determined with STRING.

IL-17A/F, IL-9), indicating an inducible inflammation-like program in tumor cells that may modulate the TME, although protein secretion remains to be confirmed. αTGG robustly suppressed ConA-driven ERK and IκB phosphorylation, reduced expression of inflammatory and EMT markers, and prevented proMMP-2 activation, consistent with attenuation of inflammation-linked invasion. VT107 produced highly similar effects (transcriptomic $r^2 = 0.87$ with αTGG), similarly inhibiting ERK/IκB phosphorylation and proMMP-2 activation and suggesting a shared anti-inflammatory signature linked to Hippo/YAP modulation. These findings support the notion that GBM cells can engage in inflammation-like signaling, which may play a pivotal role in shaping tumor behavior and interactions with immune components.

ConA-stimulated induction of the transcription of key cytokine genes in U87 GBM cells, suggests that these cells may possess a latent or inducible inflammatory signaling capacity. Although these cytokines are traditionally associated with immune cells, particularly T helper subsets, emerging evidence indicates that tumor cells can aberrantly express immune-related genes under specific stimuli, contributing to the modulation of the TME. The upregulation of these transcripts may reflect an intrinsic ability of GBM cells to engage in inflammatory crosstalk, potentially influencing immune cell recruitment, angiogenesis, or tumor progression. While protein expression and secretion remain to be confirmed, these transcriptional changes open new avenues for exploring non-canonical inflammatory pathways in GBM. Future studies should investigate whether these cytokines are translated and functionally active, which could reveal novel mechanisms of tumor-immune interaction and identify new therapeutic targets.

Inflammation and immune cell infiltration in GBM are usually described as tumor-promoting, but an alternative, controversial hypothesis argues that certain inflammatory states and immune infiltrates can act as limitans that constrain tumor growth. This perspective highlights that inflammatory signaling is context dependent: the same mediators and cells that foster proliferation, invasion, and immune suppression under chronic, low-grade inflammation can, under different timing, magnitude, or cellular composition, trigger anti-tumor effects such as cytotoxicity, senescence, or growth restriction. Reconciling the pro- and anti-tumor roles of inflammation therefore requires high-resolution, time-dependent, and cell-type-specific studies that explicitly measure functional immune activity and Hippo pathway status. Therapeutic strategies should therefore be precision-guided: selectively amplify inflammation components that restrain growth while suppressing those that facilitate invasion, immune evasion, and possibly YAP/TAZ-driven tumorigenesis.

Interestingly, ConA decreased transcripts of canonical YAP/TEAD targets (AXL, CTGF, CYR61), implying activation of upstream Hippo kinases and functional suppression of YAP output in this context; both VT107, a direct YAP/TEAD inhibitor, and αTGG converged on suppressing inflammatory gene programs and invasion, supporting a model in which modulation of YAP activity can blunt inflammation-driven pro-tumor signaling. Recently, combining temozolomide (TMZ) with a YAP inhibitor enhanced anti-tumor efficacy in GBM models,[38,39] suggesting that targeting the Hippo/YAP axis helps overcome TMZ resistance, a major clinical challenge in GBM.[40] Thus, the high degree of molecular signature overlap between VT107 and αTGG in terms of inflammatory gene suppression suggests that modulation of YAP activity, whether through upstream Hippo activation or direct inhibition of YAP/TEAD, can attenuate inflammation-associated signaling. These findings reinforce the relevance of the Hippo-YAP axis in regulating GBM inflammation and support the therapeutic potential of targeting this pathway to reshape the TME.

However, key unresolved points include protein-level confirmation of induced cytokines and identification of the direct molecular targets of αTGG and VT107 within the ERK/IκB and upstream lectin/glycoprotein receptor networks. Recommended next steps would be validation of cytokine secretion and protein changes, mapping drug targets in the ERK/IκB–Hippo axis, and testing efficacy and bioavailability in orthotopic GBM models. Taken together, these results indicate that targeting inflammation via αTGG or Hippo inhibitors may both reduce invasion and help reprogram the microenvironment to improve responses to conventional therapies and immunotherapy, warranting mechanism-driven combination studies and biomarker development to stratify likely responders.

Conclusion

This study shows that ConA triggers a robust pro-inflammatory program in U87 GBM cells and that αTGG potently suppresses these responses in a time- and dose-dependent manner, identifying αTGG as a strong anti-inflammatory candidate extendable beyond GBM models. Hippo pathway inhibitors, especially VT107, produced comparable inhibition of ConA-induced ERK/NF-κB signaling, downstream inflammatory markers, and pro-invasive readouts, and yielded a transcriptomic anti-inflammatory signature closely matching that of αTGG. Together, these results reveal a convergence between αTGG activity and Hippo/YAP pathway modulation in dampening inflammation-driven oncogenic signaling, supporting further preclinical evaluation of αTGG and Hippo inhibitors as inflammation-targeted therapies for GBM.

Abbreviations

ATCC, American type culture collection; BSA, bovine serum albumin; ConA, Concanavalin A; EMT, epithelial-to-mesenchymal transition; ERK, extracellular signal-regulated kinases; GBM, glioblastoma; IkB, inhibitor of kappa B; MAPK, mitogen-activated protein kinase; MMP, matrix metalloproteinase; SDS, sodium dodecyl sulfate; STAT3, signal transducer and activator of transcription 3; TAZ, transcriptional coactivator with a PDZ-binding domain; TME, tumor microenvironment; TMZ, temozolomide; YAP, yes-associated protein.

Data Sharing Statement

The datasets used and/or analyzed during the current study are available from the corresponding author on reasonable request.

Acknowledgments

BA holds an Institutional Research Chair in Cancer Prevention and Treatment at UQAM. The authors thank Dr Yann Pauvert (Université de Montréal, Montreal, QC, Canada) for kindly providing αTGG, and Fondation Famille Lemaire for salary support to RG.

Author Contributions

Rosalie Zilinski: Conceptualization, Data curation, Formal analysis, Investigation, Writing – review & editing, Methodology

Roger Gaudreault: Conceptualization, Formal analysis, Writing – original draft, Writing – review & editing

Borhane Annabi: Conceptualization, Data curation, Formal analysis, Funding acquisition, Supervision, Writing – original draft, Writing – review & editing

Alain Zgheib: Data curation, Investigation, Methodology, Writing – review & editing, Formal analysis, validation, Supervsion

Angélique Sabaoth Konan: Data curation, Investigation, Methodology, Writing – original draft, Writing – review & editing, Formal analysis, Software, Conceptualization

Mirolla Tadrous: Data curation, Methodology, Writing – review & editing

All authors took part in drafting, revising or critically reviewing the article; gave final approval of the version to be published; have agreed on the journal to which the article has been submitted; and agreed to be accountable for all aspects of the work.

Funding

This work was funded by a grant from the Natural Sciences and Engineering Research Council of Canada (NSERC, RGPIN-2024-04541) to BA.

Disclosure

The authors declare that they have no competing interests. This paper is based on the Master's thesis of Angélique Sabaoth Konan, and has been published on the Université du Québec à Montréal institutional website: https://archipel.uqam.ca/19249/

References

1. Li X, Gou W, Zhang X. Neuroinflammation in glioblastoma: progress and perspectives. *Brain Sci*. 2024;14(7):687. doi:10.3390/brainsci14070687
2. Roesler R, Dini SA, Isolan GR. Neuroinflammation and immunoregulation in glioblastoma and brain metastases: recent developments in imaging approaches. *Clin Exp Immunol*. 2021;206(3):314–324. doi:10.1111/cei.13668
3. Alorfi NM, Ashour AM, Alharbi AS, et al. Targeting inflammation in glioblastoma: an updated review from pathophysiology to novel therapeutic approaches. *Medicine (Baltimore)*. 2024;103(21):e38245. doi:10.1097/MD.0000000000038245
4. Landskron G, De la Fuente M, Thuwajit P, et al. Chronic inflammation and cytokines in the tumor microenvironment. *J Immunol Res*. 2014;2014:149185. doi:10.1155/2014/149185
5. Fu M, Hu Y, Lan T, et al. The Hippo signalling pathway and its implications in human health and diseases. *Signal Transduct Target Ther*. 2022;7(1):376. doi:10.1038/s41392-022-01191-9
6. Mia MM, Singh MK. Emerging roles of the Hippo signaling pathway in modulating immune response and inflammation-driven tissue repair and remodeling. *FEBS J*. 2022;289(14):4061–4081. doi:10.1111/febs.16449
7. Zhao H, Wu L, Yan G, et al. Inflammation and tumor progression: signaling pathways and targeted intervention. *Signal Transduct Target Ther*. 2021;6(1):263. doi:10.1038/s41392-021-00658-5
8. Pelly VS, Moeini A, Roelofsen LM, et al. Anti-inflammatory drugs remodel the tumor immune environment to enhance immune checkpoint blockade efficacy. *Cancer Discov*. 2021;11(10):2602–2619. doi:10.1158/2159-8290.CD-20-1815
9. Vizcaino Castro A, Daemen T, Oyarce C. Strategies to reprogram anti-inflammatory macrophages towards pro-inflammatory macrophages to support cancer immunotherapies. *Immunol Lett*. 2024;267:106864. doi:10.1016/j.imlet.2024.106864
10. Atkinson GP, Nozell SE, Benveniste ET. NF-kappaB and STAT3 signaling in glioma: targets for future therapies. *Expert Rev Neurother*. 2010;10(4):575–586. doi:10.1586/ern.10.21
11. Roy ME, Elimam R, Zgheib A, et al. A role for the Hippo/YAP1 pathway in the regulation of in vitro vasculogenic mimicry in glioblastoma cells. *J Cell Mol Med*. 2024;28(24):e70304. doi:10.1111/jcmm.70304
12. Liu-Chittenden Y, Huang B, Shim JS, et al. Genetic and pharmacological disruption of the TEAD-YAP complex suppresses the oncogenic activity of YAP. *Genes Dev*. 2012;26(12):1300–1305. doi:10.1101/gad.192856.112
13. Al-Moujahed A, Brodowska K, Stryjewski TP, et al. Verteporfin inhibits growth of human glioma in vitro without light activation. *Sci Rep*. 2017;7(1):7602. doi:10.1038/s41598-017-07632-8

14. Alomari S, Zhang I, Hernandez A, et al. Drug repurposing for glioblastoma and current advances in drug delivery - A comprehensive review of the literature. *Biomolecules*. 2021;11(12):1870. doi:10.3390/biom11121870
15. Lyne SB, Yamini B. An alternative pipeline for glioblastoma therapeutics: a systematic review of drug repurposing in glioblastoma. *Cancers (Basel)*. 2021;13(8):1953. doi:10.3390/cancers13081953
16. Ries CH, Cannarile MA, Hoves S, et al. Targeting tumor-associated macrophages with anti-CSF-1R antibody reveals a strategy for cancer therapy. *Cancer Cell*. 2014;25(6):846–859. doi:10.1016/j.ccr.2014.05.016
17. Belkaid A, Copland IB, Massillon D, et al. Silencing of the human microsomal glucose-6-phosphate translocase induces glioma cell death: potential new anticancer target for curcumin. *FEBS Lett*. 2006;580(15):3746–3752. doi:10.1016/j.febslet.2006.05.071
18. Kunnumakkara AB, Hegde M, Parama D, et al. Role of turmeric and curcumin in prevention and treatment of chronic diseases: lessons learned from clinical trials. *ACS Pharmacol Transl Sci*. 2023;6(4):447–518. doi:10.1021/acsptsci.2c00012
19. Casati G, Giunti L, Iorio AL, et al. Hippo pathway in regulating drug resistance of glioblastoma. *Int J Mol Sci*. 2021;22(24):13431. doi:10.3390/ijms222413431
20. Ortega Á, Vera I, Diaz MP, et al. The YAP/TAZ signaling pathway in the tumor microenvironment and carcinogenesis: current knowledge and therapeutic promises. *Int J Mol Sci*. 2021;23(1):430. doi:10.3390/ijms23010430
21. Totaro A, Panciera T, Piccolo S. YAP/TAZ upstream signals and downstream responses. *Nat Cell Biol*. 2018;20(8):888–899. doi:10.1038/s41556-018-0142-z
22. Ajongbolo AO, Langhans SA. YAP/TAZ-associated cell signaling - at the crossroads of cancer and neurodevelopmental disorders. *Front Cell Dev Biol*. 2025;13:1522705. doi:10.3389/fcell.2025.1522705
23. Nguyen CDK, Yi C. YAP/TAZ Signaling and resistance to cancer therapy. *Trends Cancer*. 2019;5(5):283–296. doi:10.1016/j.trecan.2019.02.010
24. Masliantsev K, Karayan-Tapon L, Guichet PO. Hippo signaling pathway in gliomas. *Cells*. 2021;10(1):184. doi:10.3390/cells10010184
25. Roy ME, Veilleux C, Paquin A, et al. Transcriptional regulation of CYR61 and CTGF by LM98: a synthetic YAP-TEAD inhibitor that targets in-vitro vasculogenic mimicry in glioblastoma cells. *Anticancer Drugs*. 2024;35(8):709–719. doi:10.1097/CAD.0000000000001627
26. Pauvert Y, Gaudreault R, Charette AB. Improved total synthesis of 1,3,6-Trigalloyl-β-D-glucose from glucose. *Synthesis*. 2023;55(15):2325–2332. doi:10.1055/s-0042-1752404
27. Roy ME, Zgheib A, Eliopoulos N, et al. A SORT1/EGFR molecular interplay as a prognostic biomarker in glioblastoma vasculogenic mimicry: implications in the transcriptional regulation of cancer stemness and drug resistance. *BMC Cancer*. 2025;25(1):1348. doi:10.1186/s12885-025-14789-3
28. Szklarczyk D, Gable AL, Nastou KC, et al. The STRING database in 2021: customizable protein-protein networks, and functional characterization of user-uploaded gene/measurement sets. *Nucleic Acids Res*. 2021;49(D1):D605–D612. doi:10.1093/nar/gkaa1074 Erratum in: Nucleic Acids Res. 2021;49(18):10800. doi: 10.1093/nar/gkab835.
29. Veilleux C, Roy ME, Annabi B. Assessing MMP-2/9 proteolytic activity and activation status by zymography in preclinical and clinical tissue samples. *Methods Mol Biol*. 2025;2918:165–176. doi:10.1007/978-1-0716-4482-9_13
30. Akla N, Pratt J, Annabi B. Concanavalin-A triggers inflammatory response through JAK/STAT3 signalling and modulates MT1-MMP regulation of COX-2 in mesenchymal stromal cells. *Exp Cell Res*. 2012;318(19):2498–2506. doi:10.1016/j.yexcr.2012.08.003
31. Desjarlais M, Pratt J, Lounis A, et al. Tetracycline derivative minocycline inhibits autophagy and inflammation in concanavalin-A-activated human hepatoma cells. *Gene Regul Syst Bio*. 2014;8:63–73. doi:10.4137/GRSB.S13946
32. Huldani H, Rashid AI, Turaev KN, et al. Concanavalin A as a promising lectin-based anti-cancer agent: the molecular mechanisms and therapeutic potential. *Cell Commun Signal*. 2022;20(1):167. doi:10.1186/s12964-022-00972-7
33. Desjarlais M, Annabi B. Dual functions of ARP101 in targeting membrane type-1 matrix metalloproteinase: impact on U87 glioblastoma cell invasion and autophagy signaling. *Chem Biol Drug Des*. 2019;93(3):272–282. doi:10.1111/cbdd.13410
34. Nanni SB, Pratt J, Beauchemin D, et al. Impact of concanavalin-A-mediated cytoskeleton disruption on low-density lipoprotein receptor-related protein-1 internalization and cell surface expression in glioblastomas. *Biomark Cancer*. 2016;8:77–87. doi:10.4137/BIC.S38894
35. Veilleux C, Khalifa J, Zgheib A, et al. Probing into the chemopreventive properties of synthetic 1,3,6-tri-O-galloyl-α-D-glucose (α-TGG) against glioblastoma and triple-negative breast cancer-derived cell models. *Curr Res Pharmacol Drug Discov*. 2025;8:100219. doi:10.1016/j.crphar.2025.100219
36. Calses PC, Crawford JJ, Lill JR, et al. Hippo pathway in cancer: aberrant regulation and therapeutic opportunities. *Trends Cancer*. 2019;5(5):297–307. doi:10.1016/j.trecan.2019.04.001
37. Kumar R, Hong W. Hippo signaling at the hallmarks of cancer and drug resistance. *Cells*. 2024;13(7):564. doi:10.3390/cells13070564
38. Tang J, Karbhari N, Campian JL. Therapeutic targets in glioblastoma: molecular pathways, emerging strategies, and future directions. *Cells*. 2025;14(7):494. doi:10.3390/cells14070494
39. Wong CLE, Kiang MYK, Leung KKG. Abstract 7207: Targeting hippo signaling pathway to overcome chemoresistance in glioblastoma. *Cancer Res*. 2024;84(6_Supplement):7207. doi:10.1158/1538-7445.AM2024-7207
40. Lee SY. Temozolomide resistance in glioblastoma multiforme. *Genes Dis*. 2016;3(3):198–210. doi:10.1016/j.gendis.2016.04.007

Journal of Inflammation Research

Dovepress
Taylor & Francis Group

Publish your work in this journal

The Journal of Inflammation Research is an international, peer-reviewed open-access journal that welcomes laboratory and clinical findings on the molecular basis, cell biology and pharmacology of inflammation including original research, reviews, symposium reports, hypothesis formation and commentaries on: acute/chronic inflammation; mediators of inflammation; cellular processes; molecular mechanisms; pharmacology and novel anti-inflammatory drugs; clinical conditions involving inflammation. The manuscript management system is completely online and includes a very quick and fair peer-review system. Visit http://www.dovepress.com/testimonials.php to read real quotes from published authors.

Submit your manuscript here: https://www.dovepress.com/journal-of-inflammation-research-journal